Investigation of the Cluster Structure of ^{9}Be by Reactions with a Deuteron Beam

B A Urazbekov[1,2,3,4]**, S M Lukyanov**[3]**, A S Denikin**[2,3]**,**
N Itaco[1]**, D M Janseitov**[5,6]**, V Burjan**[7]**, V Kroha**[7]**,**
J Mrazek[7]**, W H Trzaska**[8]**, M N Harakeh**[9]**, D Etasse**[10]**,**
I Stefan[11]**, D Verney**[11]**, K Mendibayev**[3,6]**, T Issatayev**[3]**,**
Yu E Penionzhkevich[3]**, O Bayakhmetov**[5]**, K A Kuterbekov**[5]
and T Zholdybayev[6]

[1] Dipartimento di Matematica e Fisica, Università degli Studi della Campania Luigi Vanvitelli, I-8110 Caserta, Italy
[2] Dubna State University, 141982 Dubna, Russia
[3] Joint Institute for nuclear research, 141980 Dubna, Russia
[4] Al-Farabi Kazakh National University, 050040 Almaty, Kazakhstan
[5] L N Gumilyov Eurasian National University, 010008 Astana, Kazakhstan
[6] Institute of Nuclear Physics, 050032 Almaty, Kazakhstan
[7] Nuclear Physics Institute CAS, 25068 Řež, Czech Republic
[8] Department of Physics, University of Jyväskylä, FIN-40014 Jyväskylä, Finland
[9] KVI-CART, University of Groningen, 9747 AA Groningen, The Netherlands
[10] Normandie Université, ENSICAEN, UNICAEN, CNRS/IN2P3, LPC Caen, 14000 Caen, France
[11] Institut de Physique Nucléaire, Univ. Paris-Sud, Université Paris-Saclay, F-91406 Orsay, France

E-mail: `bakytzhan.urazbekov@gmail.com`

Abstract. Angular distributions of protons, deuterons, tritons and alpha particles emitted in the d + ^{9}Be reaction at E_{lab}=19.5 and 35.0 MeV are measured. The elastic channel is analysed in the framework of both the Optical Model and the Coupled Channel approach. Two kind of optical potentials are analysed: the semi-microscopic Double Folding potential and the phenomenological Woods-Saxon potential. The deformation parameter β_2 is obtained for the transition $\frac{5}{2}^- \rightarrow \frac{3}{2}^-$ in ^{9}Be. The (d,p) and (d,t) one nucleon exchange reactions are analysed within the Coupled Reaction Channel approach in comparison with the DWBA calculations. The Spectroscopic Amplitudes for the nuclear reactions are calculated. Differential cross sections for the reaction channel ^{9}Be$(d,\alpha)^7$Li has been calculated including both the deuteron and heavy cluster ^{5}He pickup reaction mechanisms. The contributions of two-step pickup processes of the $n+p$ and $n+\alpha$ systems to cross section of the ^{9}Be$(d,\alpha)^7$Li nuclear reaction are demonstrated.

Keywords: cluster structure, optical model, CRC, DWBA, spectroscopic amplitudes, double folding, sequential transfer

1. Introduction

The cluster structure of nuclei arises from a correlated motion of nucleons inside a nucleus. In this regime a simple subgroup can be seen as a single particle. This kind of behaviour can give insights into numerous characteristics of the nucleus, as well as affect the processes of nuclear reactions. Investigation of the cluster structure in nuclei is still one of the priority problems of modern nuclear physics in connection with the intensive developments of experimental devices.

There is a row of stable nuclei exhibiting the cluster structure, but ^{9}Be is particularly worthy of attention due to the following reasons:

− stable nucleus with the low binding energies of neutron S_n=1.665 MeV, and α-particle S_α=2.462 MeV [1];

− the deformed shape reflected in the nuclear quadrupole moment, Q= +52.9 mb [2];

− the Borromean structure of the ground state;

These aspects led to take ^{9}Be as a subject for applied researches as well as fundamental studies.

Regarding nuclear technologies, ^{9}Be is a good wall material in thermonuclear devices [3, 4]. For instance, for fusion device types a value of some dozens of percent of soft wall material is expected in the case of ^{9}Be [4]. The nucleus has been chosen as it represents the best compromise based on its ability to be well split into two energetic α-particles by γ and e^-, which are efficient promoters of thermonuclear burning. Since they can be confined by electromagnetic fields and their energy affects the temperature of the burning zone.

Scattering of the simplest projectile, such as ^{1,2}H or ^{3,4}He, on a target is a standard tool for fundamental study the structure of nuclei. This method involves measuring the angular distribution of the nuclear reaction products. It is well known that the energy and angular distributions of projectile-like particles give information about internal structure of target-like nuclei.

In our previous works [5, 6, 7] the ^{3}He interaction with ^{9}Be was studied and angular distributions of the reaction products in the following exit channels: ^{3}He+^{9}Be, ^{5}He+^{7}Be, ^{5}Li+^{7}Li, ^{6}Be+^{6}He, and ^{6}Li+^{6}Li, were measured. The obtained data were analysed within the framework of the Optical Model (OM), the Coupled Channel (CC) and the distorted wave Born approximation (DWBA) approaches . The performed

analysis of the experimental data showed that the potential parameters of the exit channels were quite sensitive. Moreover, these experiments were designed to study the breakup reactions with ^{9}Be in attempt to determine contributions of the channels through the ^{8}Be+n and ^{5}He+α structure within the inclusive measurements. It was found that the ratio $2.7 \div 1$ could be assigned to the contributions of these two channels respectively. The determined value justifies that the ^{5}He+α breakup channel plays an important role as well.

Based on the Borromean structure of ^{9}Be, special attention was focused on the breakup processes resulting in the ^{9}Be(^{6}Li, ^{6}Li)^{9}Be* nuclear reaction [8, 9]. The excited nucleus ^{9}Be* can decay either directly into the $\alpha + \alpha + n$ system or through one of the unstable nuclei, such as ^{5}He and ^{8}Be. Thereby, these relatively recent experimental studies explicitly confirm the cluster structure of ^{9}Be. The calculated branching ratios show that the low lying excited states, at $E_x < 4.0$ MeV, are mostly populated with the ^{8}Be+n configuration. In other case, the ^{5}He+α configuration plays a significant role.

Another aspect of finding the cluster structure is its attandance in the nuclear reaction mechanisms. Indeed, since the papers of Detraz *et al* [10, 11], the multiparticle-multihole structures have been expected at rather low excitation energies in nuclei. In this case, it can be understood that the nucleons are transferred as a whole strongly correlated cluster, which has the internal quantum numbers of a free particle.

The interaction of deuteron and alpha particles with ^{9}Be was studied with regard to the cluster structure [12, 13] . The matter density distributions of each cluster was calculated using the three body wave function. Based on the matter density distribution function, the interaction of colliding nuclei was built within the framework of the double folding model. Approbation of the double folded potential was carried out within the optical model on elastic scattering at laboratory energies 10-30 MeV/nucleon. Then the optical potential was used for calculating one nucleon transfer reactions within the framework of DWBA. Comparison of theoretical cross sections with experimental data led to the applicability of the double folding potential based on the three body wave function.

The current work takes the responsibility to prove the cluster structure of the ^{9}Be nucleus by the example
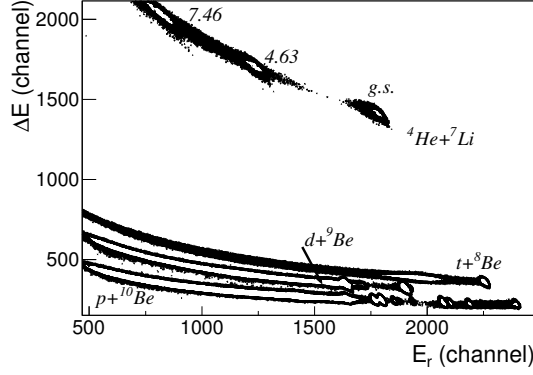
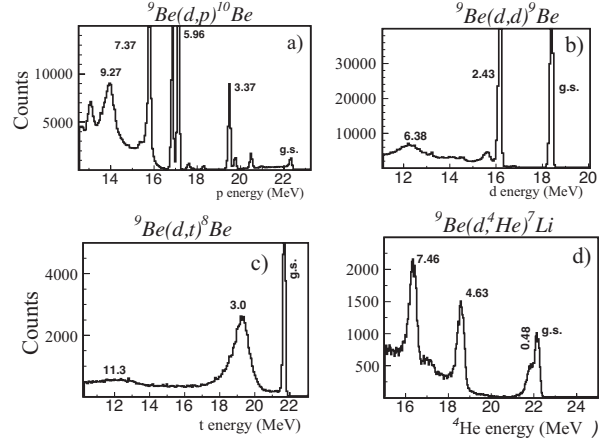**Figure 1.** Particle identification plots for the products of the ^{2}H+^{9}Be reaction: p, d, t, and ^{4}He. ΔE is the energy loss and E_r is the residual energy. Excited states for the ^{7}Li reaction channel ^{7}Li+α are indicated.

Figure 2. Total deposited energy spectra measured at θ_{lab}=32° for the detected p (panel a), d (panel b), t(panel c), and α(panel d). The ground and the excited states of ^{7}Li for the detected complementary product α as well as the ground states and the excited states for ^{8}Be, ^{9}Be, and ^{10}Be in the case of detected t, d, and p, as complementary products, respectively, are unambiguously identified.

of nuclear reactions caused by a deuteron beam at 19 MeV and 35 MeV energies. In the exit channel the simplest particles, such as p, d, t, and α-particles, were registered and their angular distributions were obtained. Regarding the previous work [13], we have extended our studies by adding the ^{9}Be(d,α)^{7}Li nuclear reaction, in which two-step processes can occur. A comparative analysis of experimental data and theoretical calculations has been performed.

2. Experimental Method

The experiment has been performed at the INP (Řež, Czech Republic) and in the Physics Department of Jyväskylä University (Jyväskylä, Finland). The beam energy of ^{2}H ions produced from the cyclotrons were at energies 19.5 and 35 MeV. The average beam current during the experiment was maintained at 20 nA. The self-supporting ^{9}Be target was prepared from a thin beryllium foil with the 99 % purity. A set of four telescopes was used with the purpose of registering the simplest particle of output channels. Each telescope was contained the ΔE$_0$, ΔE, E$_r$ detectors with the respective thickness of 12 μm, 100 μm and 3 mm. To detect reaction product in narrow divergence, telescopes were mounted at a distance of ∼25 cm from the target. Each telescope was shielded by a Cu-Pb collimator with thickness of 3 mm and hole with diameter of 3 mm. The telescopes were mounted on rotating supports, which allow us to obtain data from $\theta_{lab} = 20°$ to 107° in steps of 1-2°.

The particles were identified based on the energy-loss measurements of ΔE and the residual energy E$_r$, i.e., by the so-called ΔE-E method. An example of two-dimensional plots (yield vs. energy loss ΔE and residual energy E$_r$) is shown in Fig. 1.

The capability of current experimental technique is in identification of the particles p, d, t, and α and in the determination of their total deposited energies. The spectra of total deposited energy are shown in Fig. 2. All the peaks from Fig. 2 has been identified and assigned to the ground and the excited states of the ^{10}Be, ^{9}Be, ^{8}Be, ^{7}Li nuclei as the complementary products for the detected particles p, d, t, α, respectively.

3. Data Analysis and Results

3.1. Elastic scattering

The theoretical calculations of the deuteron elastic scattering on ^{9}Be at 19.5 and 35 MeV energies have been made in the framework of the Optical Model (OM). The model suggests interaction between two colliding nuclei in the following way:

$$U(R) = -V^V(R) - iW^V(R) + iW^D(R) + \\ + V^{SO}(R)(\mathbf{1}\cdot\sigma) + V^C(R), \quad (1)$$

where V^V, W^V, W^D, V^{SO}, and V^C are volume, imaginary volume and surface, spin-orbit and Coulomb potentials, respectively. In this work the real part of the optical potential were used in two forms, firstly the double folding potential (DF)

$$V^V(R) = N_R V^{DF}(R) \quad (2)$$

with normalization factor N_R and, secondly the phenomenological Woods-Saxon (WS) potential:

$$V^V(R) = V_0^V f^{R_V, a_V}(R), \quad (3)$$

$$f^{R_V, a_V}(R) = \frac{1}{1 + exp\frac{R-R_V}{a_V}}. \quad (4)$$
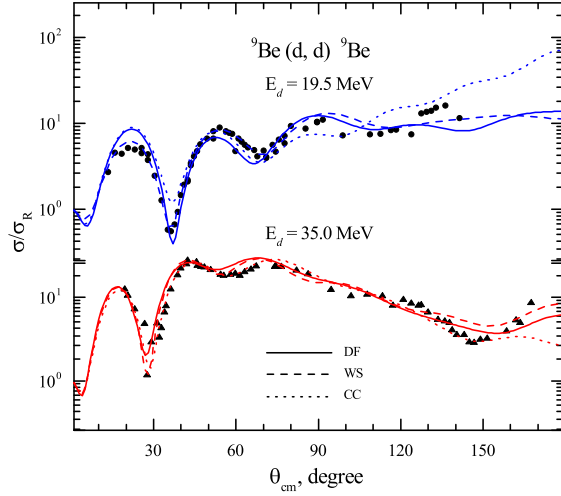
Figure 3. The angular distributions of elastic scattering data of d from ^{9}Be at laboratory energies 19.5 MeV (full circle) and 35 MeV (full triangle) in comparison with theoretical calculations within optical and couple channel model.

Figure 4. Radial dependence of the real part of the nuclear potentials used in the elastic scattering analysis.
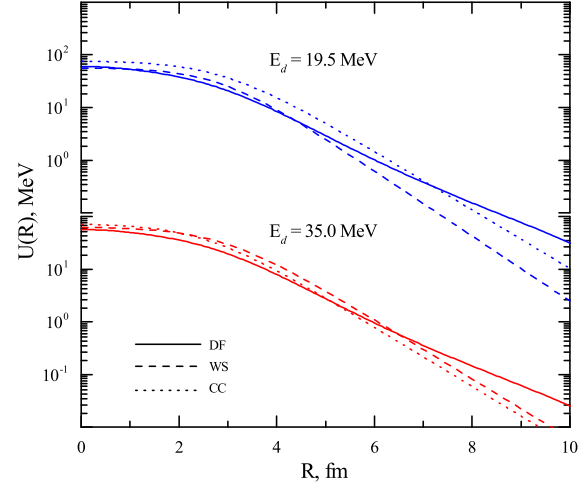
The DF potential was calculated using the effective M3Y-Paris nucleon-nucleon potential and the nuclear-matter-densities of projectile and target nuclei. Particularly we apply the three body model $\alpha + \alpha + n$ [12] in order to obtain density distribution of the ^{9}Be nucleus.

The imaginary volume term of the optical potential was also parameterized in the Wood-Saxon form as well (??? where is it in Table?), while the surface and spin-orbit terms have standard form

$$W^D(R) = -4a_D W_0^D \frac{d}{dR} f^{R_D, a_D}(R), \tag{5}$$

$$V^{SO}(R) = V_0^{SO} \left(\frac{\hbar}{m_\pi c}\right)^2 \frac{1}{R} \frac{d}{dR} f^{R_{SO} a_{SO}}(R). \tag{6}$$

This form of the imaginary component of the optical potential was used for all the forms of the real one. The Coulomb term has been taken as the interaction of a point-charge with a uniformly charged sphere

$$V^C(R) = \begin{cases} \dfrac{Z_1 Z_2 e^2}{2R_C} \left(3 - \dfrac{R^2}{R_C^2}\right) & \text{for } R \le R_C \\ \dfrac{Z_1 Z_2 e^2}{R} & \text{for } R > R_C \end{cases} \tag{7}$$

The parameters of the real and imaginary parts of the optical potential were obtained fitting the theoretical cross sections to the experimental data at 19.5 MeV and 35 MeV energies. As a starting point one of the available global parametrization [14] was used. The potential parameters obtained after fitting are listed in Table 1.

The measured elastic scattering cross sections are plotted in Fig. 3 in the scale of the ratio to Rutherford cross section in comparison with the theoretical curves corresponding to the optical model calculations using the DF potential (solid curve) and the WS potential (dashed curve). Figure 4 shows the real parts of the different nuclear potentials used here.

A specific feature of the DF potential in comparison with the empirical ones is slow descending

Table 1. Potential parameters of the d+^{9}Be system used in the OM, the CC and the DWBA calculations.

E_d MeV	The potential	V_0, fm	r_V, fm	a_V, MeV	W_D, fm	r_D, fm	a_D, MeV	V_{SO}, fm	r_C
19.5	DF		$N_R = 1.93$ [a]		14.89	0.63 [b]	0.854	5.56	0.809
	WS	57.32	0.846	0.602	7.27	0.702	1.094	−	0.809
	CC	77.87	0.87	0.78	7.92	0.816	0.802	2.8	0.809
35.0	DF		$N_R = 1.81$ [a]		14.27	0.63	0.88	5.56	0.809
	WS	64.03	0.859	0.77	14.58	0.762	0.736	−	0.809
	CC	73.9	0.75	0.77	8.93	0.816	0.802	2.8	0.809

[a] The DF potential was taken as a real volume part of the optical potential with the normalization parameter N_R.
[b] Radii of the potential were defined as $R_i = r_i \left(A_P^{1/3} + A_T^{1/3}\right)$.
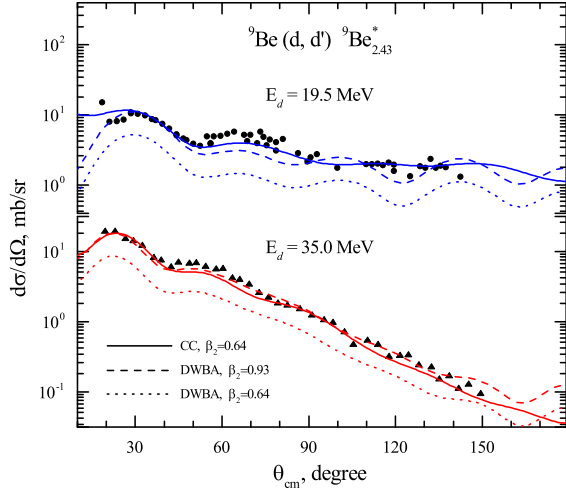
Figure 5. The cross sections of inelastic scattering ^{9}Be(d,d)^{9}Be* (E_{exc}=2.43 MeV) at laboratory energies 19.5 MeV (full circle) and 35 MeV (full triangle). Theoretical curves are described in the text.

in peripheral region $r \geq 6$ fm. This is due to the broad matter density distribution of the valence neutron in ^{9}Be, which also decreases slowly [12].

The potentials obtained in this way provide quite good description of the elastic scattering cross section.

3.2. Inelastic scattering

The CC and the DWBA approaches have been applied to analyse the inelastic scattering data corresponding to the excitation of the $J^\pi = \frac{5}{2}^-$ state with $E^* = 2.43$ MeV in the ^{9}Be target. Calculations were performed employing the *FRESCO* code [15] and the DWUCK5 code available on *NRV* knowledge-base [16].

In order to describe obtained experimental data one consider the deformed ^{9}Be nucleus having the quadrupole deformation and the main rotational band in the excitation spectrum including the ground state, $\frac{5}{2}^-$ state at 2.43 MeV and $\frac{7}{2}^-$ state at 6.38 MeV. All these states were included into the coupling scheme within the couple channel approach. The spin reorientation effects were also taken into account. The coupling interaction has the usual form:

$$V_\lambda(R) = -\beta_\lambda R_V \left| \frac{dV^V}{dR} \right| - i\beta_\lambda R_W \left| \frac{dW^D}{dR} \right|, \qquad (8)$$

where β_λ is the deformation parameter of λ multipole describing the target-nucleus form. Here we as usual neglect the contribution of the Coulomb interaction.

The calculated cross sections for inelastic scattering are shown in Fig. 5. The solid curves correspond to the results obtained within the CC approach, while the dashed and dotted curves were obtained within the DWBA approach using different values of the deformation parameter β_2. The potential used in the CC

approach was taken in a such way that reproduces the cross section of inelastic scattering as well as elastic scattering data well (see Fig. 3). The parameters of the CC potential are listed in Table 1.

All the results in Fig. 5 are in good agreement with experimental data. The quadrupole deformation parameter $\beta_2 = 0.64$ extracted within couple channel model is in consistence with the previous studies [5, 17].

In the case of DWBA calculations one use the DF potential (see Table 1) for both the entrance and the exit channels. The DWBA angular distributions very well reproduce the structure of experimental data but distinctly underestimate them when the deformation parameter $\beta_2 = 0.64$ is used (see the dotted curves in Fig. 5). In order to get the best fit the deformation parameter must be increased up to $\beta_2 = 0.93$ which is quite close to the values reported in previous studies (see, for example, [18, 19]).

Thus one may confirm that channel coupling and the effects of spin re-orientation enhance the cross section that results in the reduction of the deformation parameter. However, the DWBA approach takes into account only first order contributions to the transition amplitude and, in particular, describes only general features of the angular distributions and overestimates the deformation parameter in order to compensate the difference between the experimental data and the DWBA cross sections.

3.3. One nucleon transfer reactions

The one neutron pick-up ^{9}Be(d,t)^{8}Be and stripping ^{9}Be(d,p)^{10}Be reactions were analyzed here within the framework of both the Coupled Reaction Channels (CRC) and the DWBA approaches.

In the case of the DWBA approach the distorted
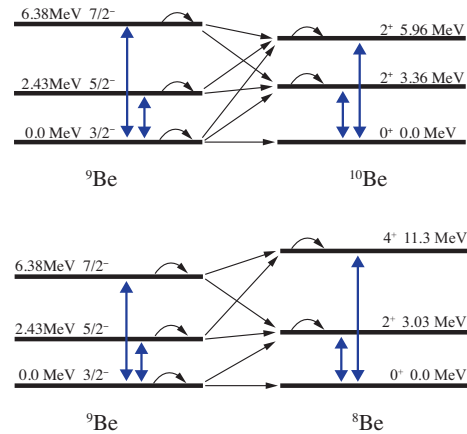
Figure 6. The target coupling schemes in the ^{9}Be(d,p)^{10}Be (upper) and the ^{9}Be(d,t)^{8}Be (lower) nuclear reactions. The bold two headed arrows indicate Eλ transitions. The spin re-orientation effects are indicated as back pointing arrows.
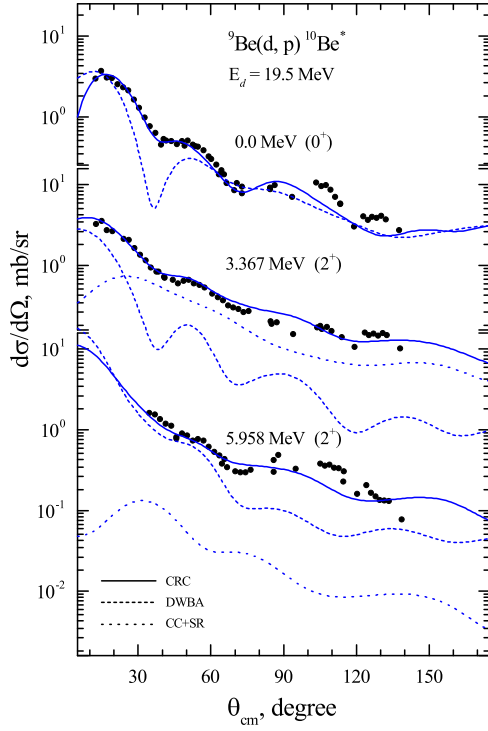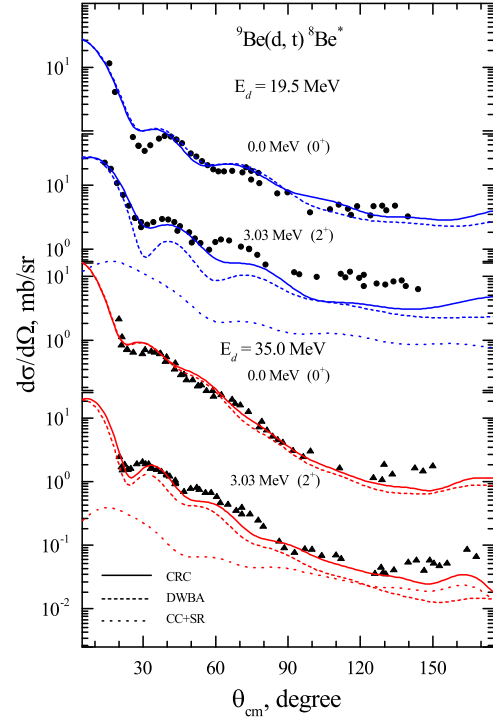
Figure 7. Differential cross sections for the ground and low-lying excited states of ^{10}Be produced in the d + ^{9}Be nuclear reaction at 19.5 MeV. Experimental data are in comparison with theoretical results obtained with the CRC and the DWBA methods.

Figure 8. Differential cross sections of the ground and low-lying excited states of ^{8}Be produced in the d + ^{9}Be reaction at both 19 MeV and 35 MeV energies. The experimental data are shown in comparison with theoretical results calculated within the CRC and the DWBA methods.

wave functions in the entrance and exit channels were calculated using the DF potential (see Table 1) and the proton [20] and triton [21] global optical potentials correspondingly. The DWBA transition amplitude in the framework of this approach has been taken in prior form for both reactions.

In order to construct the bound state wave functions of the transferred particle in entrance and exit channels one employed the common method, i.e. fitting the depth of the corresponding Woods-Saxon potential to the known binding energy. The reduced radius and diffuseness in this case are set to be equal $r = 1.25$ fm and $a = 0.65$ fm correspondingly. If the transfer takes place to the final unbound states, the depth of the potential for this state was adjusted to provide the binding energy equal to -0.1 MeV in accordance with the recommendation given in Ref. [17].

The spectroscopic amplitudes for one particle states were calculated by means of the *ANTOINE* code [22] using the effective Cohen-Kurath interaction for p-shell nuclei [23]. In particular, the spectroscopic amplitude $\mathcal{S}$ for an addition of nucleon from a specific initial state J' to a specific final state J is related to the matrix element of the creation operator $\hat{a}^\dagger$ or the

annihilation operator $\hat{a}$ [24]:

$$\mathcal{S} = \frac{\langle Jk^n \| \hat{a}^\dagger \| J'k^{n-1} \rangle}{\sqrt{2J+1}} = (-)^{j+J-J'} \frac{\langle J'k^{n-1} \| \hat{a} \| Jk \rangle}{\sqrt{2J+1}} \quad (9)$$

where symbol k stands for the set of single-particle quantum numbers $\{nlj\}$. The calculated spectroscopic amplitudes for the one nucleon transfer reactions are listed in Table 2.

The couple channel potentials given in Table 1 were used in the CRC calculations for the entrance channel. The coupling schemes of target nuclei for the ^{9}Be(d,p)^{10}Be and ^{9}Be(d,t)^{8}Be reactions are illustrated in Fig. 6. The states of ^{10}Be, 2_1^+ and 2_2^+, as well as the low-lying excited states of ^{8}Be, 2^+ and 4^+, were implemented to the coupling scheme. Also, the schemes take into account the spin reorientation effects of states on the condition $J \neq 0$.

Angular distributions of the ^{9}Be(d,p)^{10}Be and ^{9}Be(d,t)^{8}Be nuclear reactions are shown in the Fig. 7 and 8, respectively. Theoretical calculations within the CRC approach are in good agreement with experimental data. The analysis shows the importance of taking into account the channel coupling and spin reorientation effects, if one excludes the direct DWBA transitions: ^{9}Be$^{g.s.} \to ^8$Be* and ^{9}Be$^{g.s.} \to ^{10}$Be*. The contribution of these components are indicated as CC + SR in Fig. 7 and 8. *Details! Not clear...*

Table 2. Spectroscopic amplitudes used in CRC calculations for the Composite = Core + Cluster system. The one nucleon Spectroscopic Amplitudes calculated by means of the *ANTOINE* code [22]. The alpha spectroscopic amplitudes were taken from [25, 26].

Composite	$2J_{com}$	Core	$2J_{core}$	Cluster	2J	SA	Composite	$2J_{com}$	Core	$2J_{core}$	Cluster	2J	SA
^{9}Be	3	^{8}Be	0	n	3	−0.761	^{9}Be	3	^{8}Li	2_1	p	1	−0.444
^{9}Be	3	^{8}Be	4	n	3	0.816	^{9}Be	3	^{8}Li	6	p	3	−0.592
^{9}Be	3	^{8}Be	4	n	1	−0.242	^{9}Be	3	^{8}Li	2_2	p	3	−0.236
^{9}Be	5	^{8}Be	4	n	3	0.986	^{9}Be	3	^{8}Li	2_2	p	1	0.036
^{9}Be	5	^{8}Be	4	n	1	−0.417	^{9}Be	5	^{8}Li	4	p	3	0.593
^{9}Be	5	^{8}Be	8	n	3	−0.374	^{9}Be	5	^{8}Li	4	p	1	0.515
^{9}Be	7	^{8}Be	4	n	3	−0.457	^{9}Be	5	^{8}Li	2_1	p	3	−0.672
^{9}Be	7	^{8}Be	8	n	3	0.919	^{9}Be	5	^{8}Li	6	p	3	−0.571
^{9}Be	7	^{8}Be	8	n	1	−0.429	^{9}Be	5	^{8}Li	6	p	1	−0.171
^{8}Be	0	^{7}Li	3	p	3	−1.204	^{9}Be	5	^{8}Li	2_2	p	3	0.2
^{8}Be	0	^{7}Li	1	p	1	0.736	^{9}Be	7	^{8}Li	4	p	3	−0.323
^{8}Be	4	^{7}Li	3	p	3	−0.748	^{9}Be	7	^{8}Li	6	p	3	−0.899
^{8}Be	4	^{7}Li	3	p	1	−0.612	^{9}Be	7	^{8}Li	6	p	1	−0.564
^{8}Be	4	^{7}Li	1	p	3	0.667	^{7}Li	3	^{6}Li	2	n	3	0.657
^{8}Be	4	^{7}Li	7	p	3	0.624	^{7}Li	3	^{6}Li	2	n	1	−0.538
^{8}Be	4	^{7}Li	5_2	p	3	0.079	^{7}Li	3	^{6}Li	6	n	3	0.744
^{8}Be	4	^{7}Li	5_2	p	3	−0.146	^{7}Li	3	^{6}Li	4	n	3	−0.032
^{8}Be	8	^{7}Li	7	p	3	0.864	^{7}Li	3	^{6}Li	4	n	1	0.399
^{8}Be	8	^{7}Li	7	p	1	0.687	^{7}Li	1	^{6}Li	2	n	3	−0.925
^{8}Be	8	^{7}Li	5_2	p	3	0.374	^{7}Li	1	^{6}Li	2	n	1	0.197
^{8}Li	4	^{7}Li	3	n	3	−0.988	^{7}Li	1	^{6}Li	4	n	3	−0.555
^{8}Li	4	^{7}Li	3	n	1	0.237	^{7}Li	7	^{6}Li	6	n	3	−0.936
^{8}Li	4	^{7}Li	1	n	3	0.43	^{7}Li	7	^{6}Li	6	n	1	0.645
^{8}Li	4	^{7}Li	7	n	3	−0.496	^{7}Li	7	^{6}Li	4	n	3	−0.456
^{8}Li	4	^{7}Li	5	n	3	−0.665	^{7}Li	5_2	^{6}Li	2	n	3	−0.650
^{8}Li	4	^{7}Li	5_2	n	1	−0.275	^{7}Li	5_2	^{6}Li	6	n	3	0.732
^{8}Li	2_1	^{7}Li	3	n	3	0.567	^{7}Li	5_2	^{6}Li	6	n	1	0.549
^{8}Li	2_1	^{7}Li	3	n	1	0.351	^{7}Li	5_2	^{6}Li	4	n	3	0.200
^{8}Li	2_1	^{7}Li	1	n	3	0.905	^{7}Li	5_2	^{6}Li	4	n	1	−0.114
^{8}Li	2_1	^{7}Li	1	n	1	0.331	^{6}Li	2	d	2	α	0	0.907
^{8}Li	2_1	^{7}Li	5_2	n	3	0.767	^{6}Li	2	d	2	α	4	0.077
^{8}Li	6	^{7}Li	3	n	3	0.581	^{6}Li	6	d	2	α	4	0.943
^{8}Li	6	^{7}Li	5_2	n	3	−0.66	^{6}Li	6	d	2	α	8	0.028
^{8}Li	6	^{7}Li	5_2	n	1	−0.541	^{6}Li	4	d	2	α	4	0.929
^{8}Li	6	^{7}Li	7	n	3	0.973	^{9}Be	3	^{5}He	3	α	0	−0.925
^{8}Li	6	^{7}Li	7	n	1	−0.404	^{9}Be	3	^{5}He	3	α	4	0.784
^{8}Li	2_2	^{7}Li	3	n	3	−0.617	^{9}Be	5	^{5}He	3	α	4	0.974
^{8}Li	2_2	^{7}Li	3	n	1	−0.841	^{9}Be	5	^{5}He	3	α	8	−0.26
^{8}Li	2_2	^{7}Li	1	n	3	0.178	^{9}Be	7	^{5}He	3	α	4	0.882
^{8}Li	2_2	^{7}Li	1	n	1	0.331	^{9}Be	7	^{5}He	3	α	8	−0.737
^{8}Li	2_2	^{7}Li	5	n	3	0.231	^{7}Li	3	t	1	α	1	0.970
^{9}Be	3	^{8}Li	4	p	3	−0.947	^{7}Li	1	t	1	α	1	0.961
^{9}Be	3	^{8}Li	4	p	1	−0.319	^{7}Li	7	t	1	α	3	0.952
^{9}Be	3	^{8}Li	2_1	p	3	0.454	^{7}Li	5_2	t	1	α	3	0.223

The theoretical analysis given in Ref. [27] demonstrates the dominance of two-step transfer mechanism in case of ^{9}Be(d,p)^{10}Be reaction at $E_d = 15$ MeV. It was shown that the sequential neutron pickup and dineutron stripping provide the main contribution to the cross section at the forward scattering angles, while the neutron stripping and the ^{8}Li-cluster pick-up give the cross section at scattering angles $\theta_{c.m.} > 50°$.

Our results confirm *(?)* these conclusions and provide impressive agreement with the experimental data. *What do our results say?*

Thus one may conclude, *(?)* the results obtained within the CRC approach to the ^{9}Be(d,p)^{10}Be and ^{9}Be(d,t)^{8}Be reactions, including the excited states and spin reorientations, indicate the strong coupling channel effects in both entrance and exit channels. The effects of such kind were also emphasized in Ref. [17, 28].

3.4. Cluster transfer reaction

Differential cross sections for the nuclear reaction ^{9}Be(d,α)^{7}Li are of particular interest. The reason is in specific behaviour of the cross section at large scattering angles, that shows possibility for the ^{5}He cluster transfer. In addition, the cross section
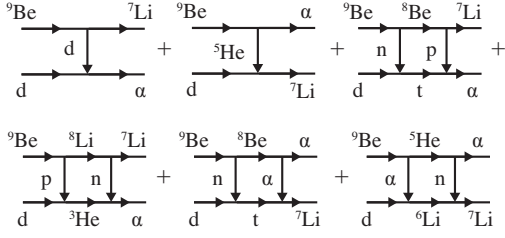
Figure 10. The scheme illustrates the reaction mechanisms taken into account in CRC calculations of the cross sections for $^9\mathrm{Be}(d,\alpha)^7\mathrm{Li}$ reaction.

calculated within the DWBA approach underestimates data even at forward scattering angles. Therefore, in order to cure the distinction between theory and experiment, the following transfer mechanisms are suggested (see Fig. 10):

– direct transfer of heavy clusters d and $^5\mathrm{He}$;

– sequential two-step transfer of n-p, p-n, n-α and α-n;

The resulting differential cross section for the $^9\mathrm{Be}(d,\alpha)^7\mathrm{Li}$ reaction has form of a coherent sum of two amplitudes

$$\frac{d\sigma}{d\Omega}(\theta) = |f_I(\theta) + f_{II}(\theta)|^2, \qquad (10)$$

where the amplitude

$$f_I(\theta) = f_{^5\mathrm{He}}(\pi - \theta) + f_{n-\alpha}(\pi - \theta) + f_{\alpha-n}(\pi - \theta) \quad (11)$$

describes the transfer of the heavy $^5\mathrm{He}$-cluster and sequential two-step transfer of n-α and α-n, and the amplitude

$$f_{II}(\theta) = f_d(\theta) + f_{n-p}(\theta) + f_{p-n}(\theta) \qquad (12)$$

corresponds to the deuteron pick-up and sequential two-step transfer of n-p and p-n.

This paragraph seems to be unnecessary... The quantum numbers of transferred clusters NL_J have been constructed by conservation of the total number of oscillation quanta $\mathcal{N}$ [29]

$$\mathcal{N} = 2(N-1) + L = \sum_i \left(2\left(n_i - 1\right) + l_i\right), \qquad (13)$$

where $i-$ the number of each constituent nucleon in the cluster, $n_i l_i-$ the quantum numbers of i-indexed nucleon, and by the triangle law of inequality:

$$|J_{com} - J_{core}| \le J \le |J_{com} + J_{core}|, \qquad (14)$$

where J_{com}, J_{core} are the spin numbers of composite and core nuclei, respectively.

The CC potential (see Tab. 1) for the entrance channel and global optical potential parameterizations from Ref. [21, 30, 31] for intermediate and exit
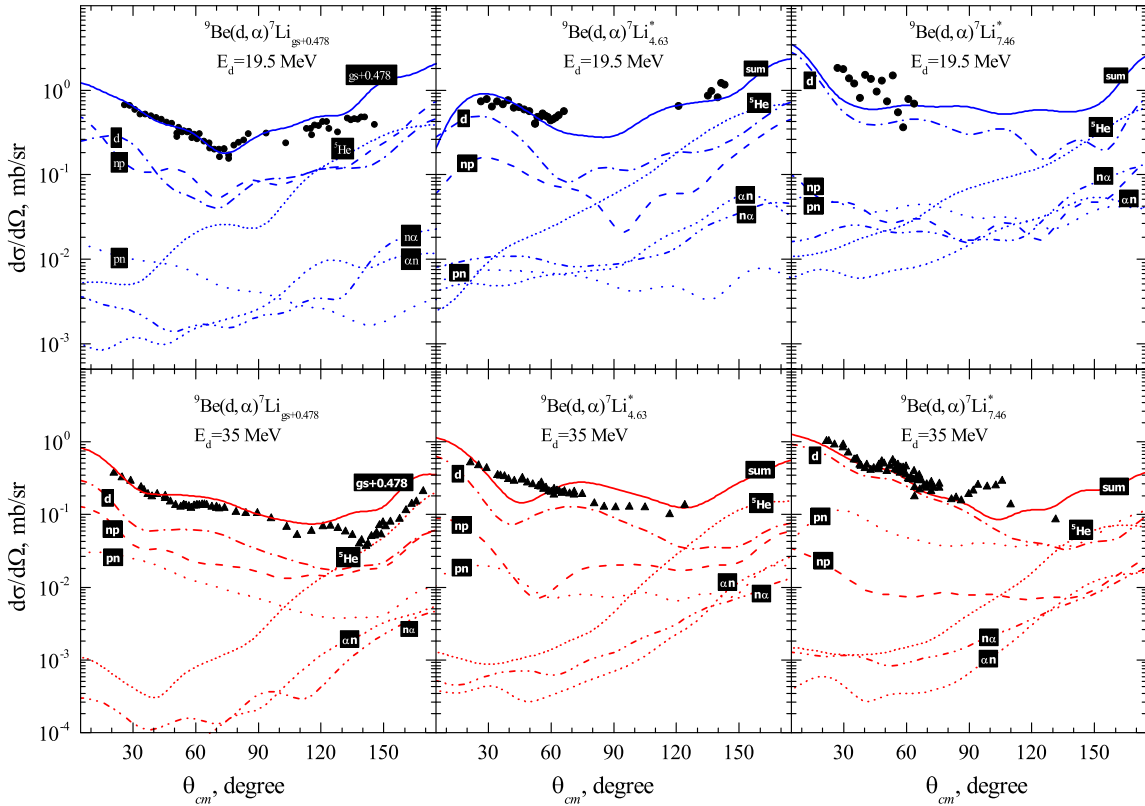
Figure 9. Differential cross sections for the ground and low-lying excited states of $^7\mathrm{Li}$ produced in the d + $^9\mathrm{Be}$ reaction at both 19.5 MeV and 35 MeV.

channels were used in analysis. For two-step transfer reactions the transition amplitudes were calculated in the prior form for the first coupling, and in the post form for the second coupling.

Important ingredients of the CRC method are the spectroscopic amplitudes of the composite configurations in the entrance, exit and intermediate states. In order to calculate the one nucleon spectroscopic amplitudes we applied the *ANTOINE* code [22] that ... *(some explanations of the code details are needed)*

The spectroscopic amplitudes of the d and ^{5}He clusters were taken from Ref. [32], while the alpha-cluster spectroscopic amplitudes given in Tab. 2 were provided by Dr. A. Volya within the method reported in Ref. [26].

Figure 9 shows the α-particle angular distributions formed in the ^{9}Be(d,α)^{7}Li* reaction at energies 19.5 and 35 MeV and corresponding to the low-lying excitation of the ^{7}Li nucleus in exit channels. Fig. 9 shows that in all the channels the transfer of the deuteron provides the dominant contribution. Despite the fact that the spectroscopic amplitude of the deuteron 0.558 within $1D_3$ state [18] in the ^{9}Be nucleus is not of great importance, a noticeable cross section is due to the large value of the deuteron spectroscopic amplitude 1.732 in the configuration $1S_1$ of ^{4}He.

It should be noted that the contribution of the deuteron transfer mechanism to the cross section mainly occurs with the wave $1D_3$ in the background with other waves, such as $2S_1, 1D_1, 1D_2$. *(it is not clear...)*

It is important to note that the behaviour of the $1D_3$ wave converges very slowly with respect to the angle, which is almost identical to the angular distribution of evaporation residues. *what does it mean: wave converges... ?*

In all channels starting from scattering angle $\theta_{c.m.} = 120°$ the transfer of the ^{5}He cluster has a predominant contribution. It is interesting to note that the the ^{5}He-cluster transfer has one-step mechanisms in all the exit channels as it was mentioned early in Ref. [18]. In this paper, an analysis of the nuclear reaction at $E_{lab} = 7$ MeV was performed supposing the simultaneous ^{5}He cluster transfer, and neglecting the sequential transfer *(and what the results?)*.

Using the CRC method, we are able to estimate the contribution of the sequential transfer of the ^{5}He, which was not studied before. Corresponding cross sections are shown in Fig. 9 as curves labeled $n\alpha$ and αn. It turned out that the $n\alpha$ and the αn transfer processes provide indeed the contribution more than one order of magnitude lower in comparison with the one-step ^{5}He transfer. One-step transfer of the ^{5}He cluster was also indicated as a dominant process by Jarczyk *et al* [33] studing the ^{12}C(^{11}B,^{6}Li)^{17}O and
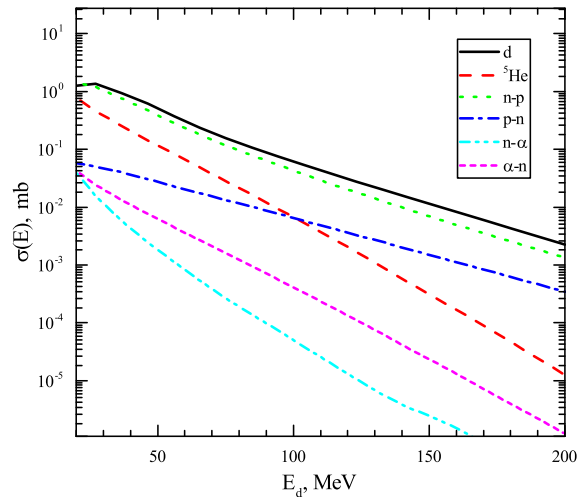
Figure 11. Integrated cross sections depending on laboratory energy E_d for each mechanism: d, ^{5}He, n-p, p-n, n-α and α-n.

^{12}C(d,^{7}Li)^{7}Be reactions. Nevertheless, it should be noted that the contribution of the n-α and the α-n transfer channels increase with the ^{7}Li excitation increases, where they should not be ignored.

The two-step n-p transfer is another mechanism providing noticeable contribution to the cross section. It is due to the prominent cluster structure of the ^{9}Be nucleus having the weakly bound neutron. This structural feature explains also the weakness of the p-n transfer contribution since the proton separation energy for the ^{9}Be isotope exceeds the neutron one more than 10 times.

This conclusion is in agreement with previous results reported in particularly in Ref. [34]. In this paper, the treatment of the DWBA discrepancy in the ^{98}Mo(d,α)^{96}Nb direct deuteron transfer reaction was gained by coherently adding the two-step processes. In particular, the calculations have shown that the (d,t;t,α) process prevails over the (d,^{3}He;^{3}He,α) process.

Figure 11 shows the results of calculations of the integrated cross sections for each mechanism in the ^{9}Be(d,α)^{7}Li nuclear reaction. The contribution to the cross section can be made in the following order: direct transfer of the deuteron, transfer of the n-p system, transfer of a heavy ^{5}He cluster, and sequential transfer of the p-n, a-n, and n-a systems. However, the order of the contribution of the p-n and ^{5}He mechanisms changes when the laboratory energy reaches a value of 100 MeV.

4. Conclusion

In the present work, the nuclear reactions induced by interaction of deuteron with ^{9}Be have been analysed. The following conclusions can be made during the

analysis:

- The double-folding potential, which is characteristic of the interaction of deuteron with ^{9}Be, differs from phenomenological optical potentials;

- The deformation parameter has been obtained for the excited state 2.43 MeV of ^{9}Be;

- The strong coupling effects in the nuclear reactions with one nucleon transfer have been revealed;

- It was found that in the ^{9}Be(d,α)^{7}Li nuclear reaction the ^{5}He heavy cluster is transferred mainly simultaneously, and the contribution of its sequential transfer is an order of magnitude lower;

- The importance of taking into account the mechanism of sequential transfer of the n-p system has been revealed.

Acknowledgments

References

[1] Wang M, Audi G, Wapstra A H, Kondev F G, MacCormick M, Xu X and Pfeiffer B 2012 *Chin.Phys.C* **36** 1603
[2] Sundholm D and Olsen J 1991 *Chem.Phys.Lett.* **177** 91
[3] Kukulin V I and Voronchev V T 2010 *Phys.Atomic Nuclei* **73** 1376
[4] Seksembayev Z, Kukulin V and Sakhiyev S 2018 *Physica Scripta* **93** 085602
[5] Lukyanov S M, Denikin A S, Voskoboynik E I, Khlebnikov S V, Harakeh M N, Maslov V A, Penionzhkevich Y E, Sobolev Y G, Trzaska W H, Tyurin G P and Kuterbekov K A 2014 *J.Phys.(London)* **G41** 035102
[6] Lukyanov S M, Harakeh M N, Naumenko M A, Xu Y, Trzaska W H, Burjan V, Kroha V, Mrazek J, Glagolev V, Piskor S, Voskoboynik E I, Khlebnikov S V, Penionzhkevich Y E, Skobelev N K, Sobolev Y G, Tyurin G P, Kuterbekov K and Tuleushev Y 2015 *World Journal of Nuclear Science and Technology* **5** 265
[7] Janseitov D M, Lukyanov S M, Mendibayev K, Penionzhkevich Y E, Skobelev N K, Sobolev Y G, Kuterbekov K A, Valiolda D S, Zholdybayev T K, Trzaska W H, Khlebnikov S V, Tyurin G P, Urazbekov B A, Harakeh M N, Burjan V, Kroha V, Mrazek J, Piskor S, Sivacek I and Glagolev V 2018 *Int.J.Mod.Phys.* **E27** 1850089
[8] Brown T A D, Papka P, Fulton B R, Watson D L, Fox S P, Groombridge D, Freer M, Clarke N M, Ashwood N I, Curtis N, Ziman V, McEwan P, Ahmed S, Catford W N, Mahboub D, Timis C N, Baldwin T D and Weisser D C 2007 *Phys.Rev. C* **76** 054605
[9] Papka P, Brown T A D, Fulton B R, Watson D L, Fox S P, Groombridge D, Freer M, Clarke N M, Ashwood N I, Curtis N, Ziman V, McEwan P, Ahmed S, Catford W N, Mahboub D, Timis C N, Baldwin T D and Weisser D C 2007 *Phys.Rev. C* **75** 045803
[10] Detraz C, Duhm H H and Hafner H 1970 *Nucl.Phys.* **A147** 488
[11] Detraz C, Pougheon F, Bernas M, Langevin M, Roussel P and Vernotte J 1974 *Nucl.Phys.* **A228** 39
[12] Urazbekov B A, Denikin A S, Sakhiev S K and Burtebaev N T 2016 *Bull.Rus.Acad.Sci.Phys.* **80** 247
[13] Urazbekov B A, Denikin A S, Sakhiev S K and Lukyanov S M 2017 *Bull.Rus.Acad.Sci.Phys.* **81** 690
[14] An H and Cai C 2006 *Phys.Rev. C* **73** 054605
[15] Thompson I J 1988 *Computer Physics Reports* **7** 167 – 212
[16] Karpov A, Denikin A, Naumenko M, Alekseev A, Rachkov V, Samarin V, Saiko V and Zagrebaev V 2017 *Nuclear Instruments and Methods in Physics Research Section A: Accelerators, Spectrometers, Detectors and Associated Equipment* **859** 112 – 124
[17] Harakeh M N, Van Popta J, Saha A and Siemssen R H 1980 *Nucl.Phys.* **A344** 15
[18] Szczurek A, Bodek K, Krug J, Lubcke W, Ruhl H, Steinke M, Stephan M, Kamke D, Hajdas W, Jarczyk L, Kamys B, Strzalkowski A and Kwasniewicz E 1989 *Z.Phys.* **A333** 271
[19] Votava H J, Clegg T B, Ludwig E J and Thompson W J 1973 *Nucl.Phys.* **A204** 529
[20] Koning A J and Delaroche J P 2003 *Nucl.Phys.* **A713** 231
[21] Li X, Liang C and Cai C 2007 *Nucl.Phys.* **A789** 103
[22] Caurier E, Martínez-Pinedo G, Nowacki F, Poves A and Zuker A P 2005 *Rev. Mod. Phys.* **77**(2) 427–488
[23] Cohen S and Kurath D 1965 *Nucl.Phys.* **73** 1
[24] Brown A 2017 *Lecture Notes in Nuclear Structure Physics* (Michigan State University)
[25] Volya A *Private communication. Unpublished*
[26] Kravvaris K and Volya A 2017 *Phys.Rev.Lett.* **119** 062501
[27] Galanina L I and Zelenskaya N S 2012 *Physics of Part.and Nuclei* **43** 147
[28] Rudchik A T, Chercas K A, Kemper K W, Rusek K, Rudchik A A, Herashchenko O V, Koshchy E I, Pirnak V M, Piasecki E, Trzcinska A, Sakuta S B, Siudak R, Strojek I, Stolarz A, Ilyin A P, Ponkratenko O A, Stepanenko Y M, Shyrma Y O, Szczurek A and Uleshchenko V V 2016 *Nucl.Phys.* **A947** 161
[29] Satchler G 1983 *Direct Nuclear Reactions* International series of monographs on physics (Clarendon Press) ISBN 9780198512691
[30] Avrigeanu V, Hodgson P E and Avrigeanu M 1994 *Phys.Rev.* **C49** 2136
[31] Cook J 1982 *Nucl.Phys.* **A388** 153
[32] Kwasniewicz E and Jarczyk L 1985 *Nucl.Phys.* **A441** 77
[33] Jarczyk L, Kamys B, Kistryn M, Magiera A, Rudy Z, Strzalkowski A, Barna R, D'Amico V, De Pasquale D, Italiano A and Licandro M 1996 *Phys.Rev.* **C54** 1302
[34] Coker W R, Udagawa T and Comfort J R 1974 *Phys.Rev.* **C10** 1130
[35] CANAM URL http://canam.ujf.cas.cz/